Title
A COMPARISON OF VELOCITY AND SCALAR SPECTRA IN PREMIXED TURBULENT FLAMES

Authors
Cheng, R.K.
Shepherd, I.G.
Gokalp, I.

Publication Date
1987-05-01

Lawrence Berkeley Laboratory
UNIVERSITY OF CALIFORNIA

APPLIED SCIENCE DIVISION

Presented at the 6th Symposium on Turbulent Shear Flow, Toulouse, France, September 7–9, 1987

A COMPARISON OF VELOCITY AND SCALAR SPECTRA IN PREMIXED TURBULENT FLAMES

R.K. Cheng, I.G. Shepherd, and I. Gokalp

May 1987

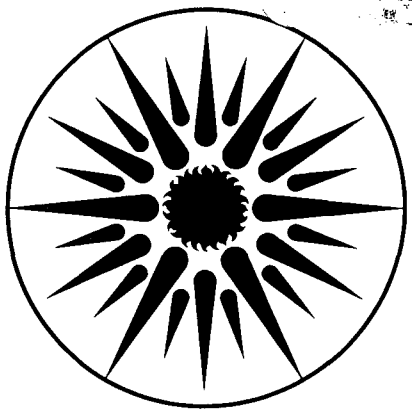

APPLIED SCIENCE DIVISION

Prepared for the U.S. Department of Energy under Contract DE-AC03-76SF00098

DISCLAIMER

A Comparison of Velocity and Scalar Spectra in Premixed Turbulent Flames

R. K. Cheng

Applied Science Division, Lawrence Berkeley Laboratory,
University of California, Berkeley CA 94720

I. G. Shepherd

Department of Mechanical Engineering
University of California, Berkeley CA 94720

and

I. Gokalp

CRCCHT - CNRS
45071 Orleans Cedex 2, France

ABSTRACT

Scalar (intermittency) and velocity spectra in premixed methane/air turbulent v-flames and stagnation flow stabilized flames have been measured using laser light Mie scattering and laser Doppler anemometry techniques. To compare the velocity spectra of the oblique v-flame with those of the normal stagnation flames, the velocity data for v-flames are transformed to obtain the spectra of the velocity components normal and tangential to the oblique flame zone. In both configurations, the spectra of the normal velocity components are similar to the corresponding scalar spectra. The most energetic frequencies are consistent with the flame passage frequencies demonstrating clearly that the velocity and scalar spectra are strongly coupled. However, the most energetic frequencies are about an order of magnitude higher in the v-flame than in the stagnation flames even though the incidence turbulence of the two flames are similar. Since this difference does not seem to be proportional to the difference in the mean velocities, our results imply that the spatial scales in the two flame zones are not the same.

NOMENCLATURE

$\bar{c}$	progress variable
$\tilde{c}$	Favre averaged conserved scalar
E	spectral distribution
l	integral length scale
L	position of stagnation plate 75 mm
n	fluctuation frequency
n_e	most energetic frequency
R_e	Reynolds number
S_L	laminar burning speed
U, u′	mean and rms axial velocity
V, v′	mean and rms transverse velocity
x	axial distance
y	transverse distance
ϕ	equivalence ratio
Ω	intermittency

Subscripts

l	based on integral length scale
L	laminar condition
n	normal to flame zone
t	tangential to flame zone
∞	free stream

INTRODUCTION

Although spectral analysis has proved a powerful tool for studying non-reacting turbulent shear flows, its application in the investigation of turbulent combustion has been limited. One reason is that, in general, experimental studies of turbulent combustion have emphasized the collection of time mean statistical quantities of scalar and velocity components for comparison with numerical model predictions. Since most of the theoretical models do not consider temporal fluctuations, the scalar and velocity spectra are sometime reported but often not analyzed in detail. With the development of recent theoretical models which place more emphasis on the temporal characteristics of the scalar and velocity fluctuations (1), experimental investigation of their spectral behavior would be useful to further the development of turbulent combustion theories and to infer the physics of the turbulence-combustion interaction processes which control the overall reaction rate.

In our previous study of velocity spectra obtained rod-stabilized premixed turbulent v-flames (2), we have shown that the features of the velocity spectra measured in the center of the flame brush for four ethylene/air flames do not seem to correlate strongly with the turbulent Reynolds number. This lack of correlation suggests that the turbulence parameters of the approach flow are insufficient to describe flame spectra. Other parameters pertaining to the turbulent flame such as the passage frequencies of the wrinkled turbulent flame structures may be important for the interpretation of the velocity spectra.

Within the wrinkled laminar flame regime for premixed turbulent flames with incident turbulence Reynolds number based on integral length scale R_l of less than 100, the flamelet model can be used to described the turbulent flame structures (3). This model is based on the concept of a thin wrinkled fluctuating flame sheet (flamelet) which separates the the unburned reactants from the burned products. In the limit when the turbulent flame brush thickness is large compared to the laminar flame thickness, the scalar and velocity statistics can be expressed by the intermittency model (4). The flame intermittency factor, Ω, is the probability of encountering the products in the flow field and can also be interpreted as the inverse mean normalized density. It is therefore identical to the conserved scalar $\bar{c}$ used in theoretical models (1). Previous studies in premixed turbulent v-flames (4) have shown that the turbulence fluctuations within the flame brush consist of rms contributions from the reactants and the products weighted respectively by $(1-\bar{c})$ and $\bar{c}$. In addition, since combustion induces expansion which accelerates the flow across the flamelet, conditioned mean velocities of the two zones are different. Each flame passage then results in a sudden change in velocity which also contributes to the rms intensities. Consequently, the velocity spectra in the flame region should also include spectral information of the fluctuating flamelet due to this velocity jump. The objective of this work is to study the effect of the flame passage frequencies on velocity spectra by comparing the velocity and scalar spectra obtained in premixed turbulent flames of different configurations.

EXPERIMENTAL SET-UP AND DATA ANALYSIS

Two idealized flame configurations are used in this study. They are 1) rod-stabilized oblique v-flames (5) and 2) turbulent flame stabilized in a stagnation flow (6). The turbulent flame brushes of these configurations are assumed to be planar and two dimensional. The characteristics of the scalar and velocity fields

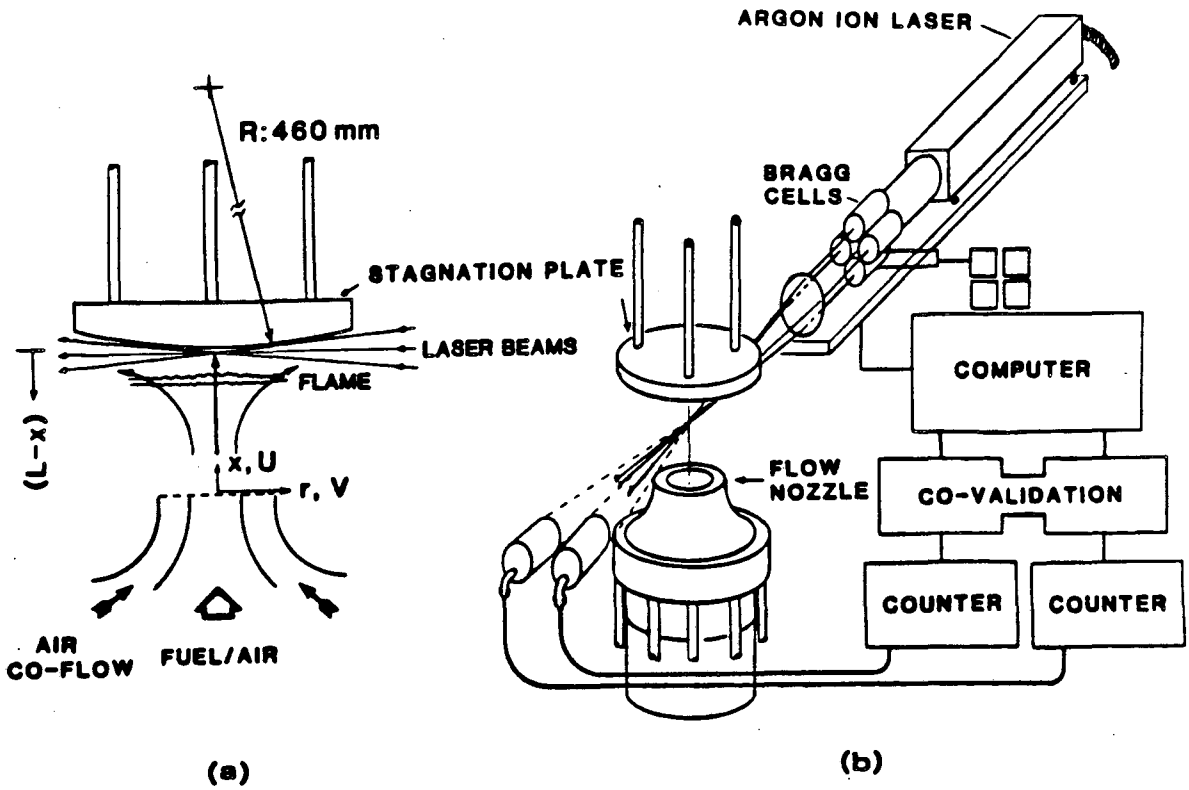

Fig. 1 Schematics of the stagnation flow stabilized turbulent flame and the LDA data acquisition system.

within the flame zones have been studied in previous works and are relatively well understood. A schematics of the stagnation flow stabilized flame configuration and the data acquisition system is shown in Figure 1. The diameter of the inner fuel/air jet is 50 mm and the diameter of the outer co-flow air jet is 100 mm. Incident turbulence is generated either by a square grid or a perforated plate placed 50 mm upstream of the nozzle exit. The stagnation plate is placed 75 mm downstream. At the nozzle exit, the turbulence intensity produced by the grid is approximately 5% while that produced by the perforated plate is 8%.

One of the most significant features of the stagnation flow stabilized flame configuration is that along the centerline, the turbulent flame brush is normal to the incident flow. It is thus closest to the idealized one dimensional flame for which many theoretical model has been developed. Another feature is that flame stabilization is not dependent on a recirculation zone and therefore the development of the wrinkled flame structures would not be influenced by the fluid mechanics of the stabilization region. To stabilize the v-flame, the stagnation plate is removed and a 1 mm diameter rod is place at the nozzle exit. Since the flame brush of the v-flame is oblique to both the principal axis of the burner and the diagnostics, to compare the results obtained for the two configurations, transformation of the v-flames velocity data to the coordinate normal to the local flame brush orientation is necessary (7).

Four sets of data have been obtained, two for each configuration using the two turbulence generators (Table I). The methane/air mixture flow and equivalence ratio conditions of the four flames are the same with $U_\infty = 5.0$ m/s ,$\phi = 0.98$. Under these flow conditions, the integral length scale of the incident turbulence at the exit of the nozzle is 2.0 mm for the grid and 3.0 mm for the perforated plate. Therefore, the turbulent flames studied here fall within the wrinkled laminar flame regime where the incident turbulence wrinkles the flame sheet without altering the internal structure of the thin reacting flamelet.

A four-beam two color laser Doppler anemometry system is used for measuring the velocity statistics of two velocity components and their spectra. All four beams were frequency shifted by Bragg cells and differential frequency of 5.0 MHz is used for both components to remove directional ambiguity. The LDA system were arranged to measure velocity components parallel (U) and perpendicular (V) to the burner axis. The Doppler bursts are analyzed by two frequency counters. Mean and rms profiles in the stagnation flow stabilized flames were measured along the centerline. For the v-flames, transverse profiles were obtained at 30 and 40 mm above the burner exit.

The velocity spectra in the stagnation flow stabilized flames were analyzed by fast Fourier transform (FFT) directly from the LDA analog output digitized at 4 kHz. To reduce the spectral noise, 100 spectra each consisting of 512 samples were averaged. Continuous sampling is justified because typical data rates in the reactants for each component approachs 25 kHz. To obtain the spectra for the velocity components normal U_n and tangential U_t to the v-flames, the outputs of the two counters are digitized simultaneously at 4 kHz and stored on magnetic tape for subsequence coordinate transformation and spectral analysis. At each measurement location within the flame zone, 20480 pairs of instantaneous velocity vectors in two dimension are recorded. The spectra for the velocity components before and after co-ordinate transformation are based on the average of 40 spectra of 512 samples. The flame coordinate for transformation is deduced from the joint probability density function of the velocity components. As shown by Cheng (5), the joint pdf is bimodal with two peaks pertaining to the reactants and the products zones. A line joining the two peaks on the U, V hodographic plan represents the axis normal to the flame. The procedure to transform the velocity data is described in (7).

Table I

flame #	configuration	$\frac{u'}{S_L}$	turbulence generator	l (mm)	Re_l
1	v	.89	plate	3.0	84
2	v	.53	grid	2.0	32
3	stagnation	.89	plate	3.0	84
4	stagnation	.55	grid	2.0	32

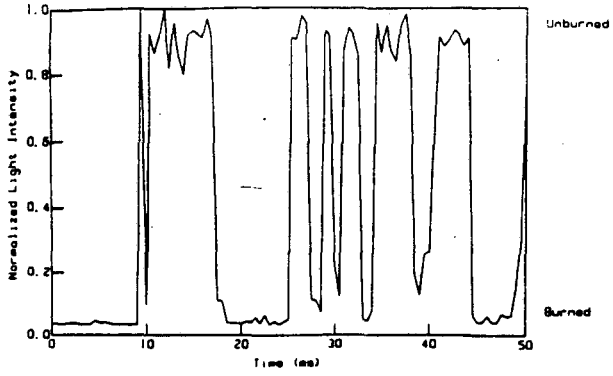

Fig. 2 Typical Mie scattering data at the middle of the turbulent flame brush.

The conserved scalar $\bar{c}$ or the flame passage frequency spectra are obtained from time resolved measurements of the flame intermittency Ω (8). The diagnostic method is quite simple: it involves measuring laser light Mie scattering intensity from silicon oil aerosol seeded in the flow; the same seeding technique used for LDA measurement of conditional velocities (5,8). Since the oil droplets evaporate and disappear through the thin wrinkled flame sheet, the output signal from the photomultiplier which is focussed on a small segment of the laser beam at the waist resembles that of a telegraph signal (Figure 2). Each passage of a flamelet is represented by a jump from burned to unburned conditions or vise versa. The spectral distribution functions of the Mie scattering signal therefore contain the information of the flamelet passage frequencies. The Mie scattering signal is digitized at 10 kHz and again 50,000 samples are used to obtain 100 spectra for averaging.

It should be noted that the application of the present Mie scattering technique to study flame intermittency assumes a priori that the flames satisfy the criteria of the intermittency or interface model which assume zero flame thickness. Another interesting feature of this technique is that compare to Rayleigh scattering (9) which measures gas density, the Mie scattering technique offer better signal to noise ratio and larger dynamic frequency range. This is because the Rayleigh scattering is much weaker than Mie scattering and so the comparatively large background radiation makes density fluctuations higher than 3 kHz difficult to resolve.

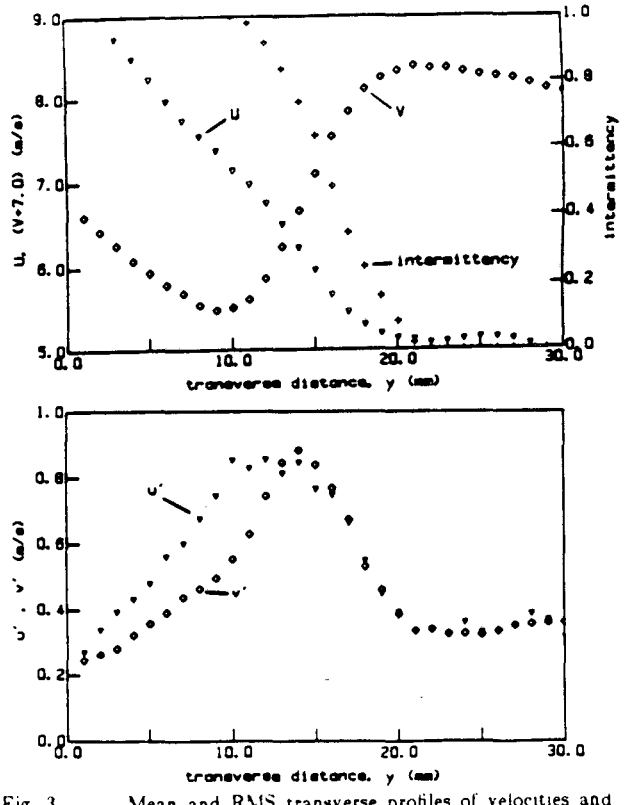

Fig. 3 Mean and RMS transverse profiles of velocities and intermittency in Flame 1 at x = 40.0 mm above the flow nozzle exit.

RESULTS AND DISCUSSION

Representative mean and rms profiles measured in the v-flame (flame 1) and stagnation flames (flame 3) are shown in figures 3 and 4 respectively. The overall features of these profiles have been discussed in detail elsewhere (5,6) and will not be repeated here. The main difference in the mean velocity profiles is that the approach flow for the v-flames is constant while the flow velocity in the stagnation flame decreases linearly towards the flame zone. As shown int Fig. 4(a), the mean velocity at the flame zone is only about 1.5 m/s compared to 5 m/s at the nozzle exit. Measurements in the turbulent stagnation flow with no combustion indicate that even though the mean flow velocity decreases, the fluctuation intensities remains constant. Moreover, the integral time scales also scale inversely with the mean velocity which imply that the integral length scale is constant. Under the same mixture and incident flow conditions, the main difference between the two type of flames is that the flame brush thickness of the stagnation flame as shown by comparing the intermittency profiles is larger. However, it should be noted that in v-flames the flame brush thickness increases with distance from the flame stabilizer. Therefore, it is difficult to determine from these sets of data the physical significance of the difference in the thickness of the v-flame and the stagnation flame.

In Fig. 3, the v' profile peaks almost at the middle of the flame brush near $\bar{c} = 0.5$ while the u' peak is located closer to the products zone. However, throughout the reactants region and up to the middle of the flame, u' and v' are identical which indicates a quasi-isotropic turbulence behavior. In contrast, only u' peaks within the stagnation flame and v' increases gradually towards the stagnation plate. Another dissimilar feature with the v-flame data is that the turbulence at the cold flame boundary is slightly anisotropic.

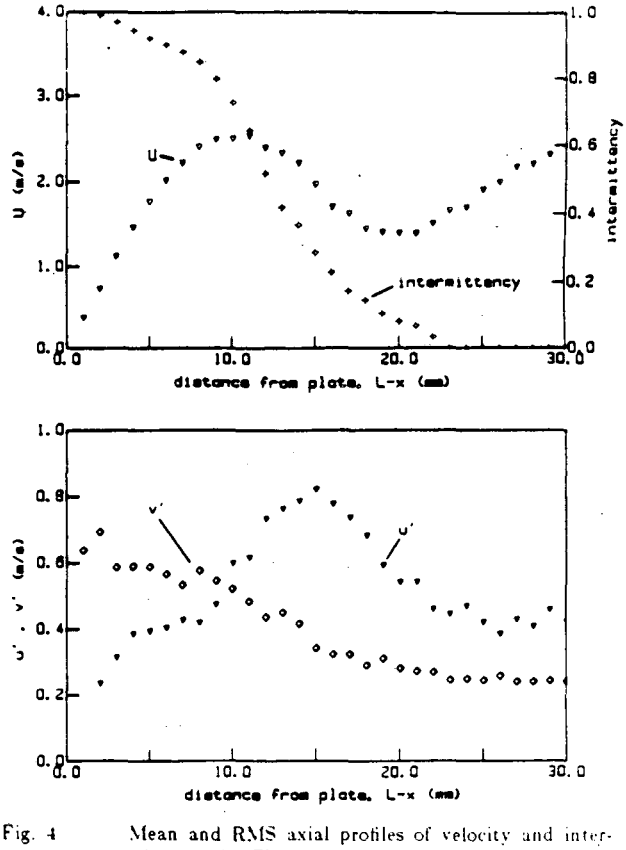

Fig. 4 Mean and RMS axial profiles of velocity and intermittency in Flame 3 along the centerline of the burner.

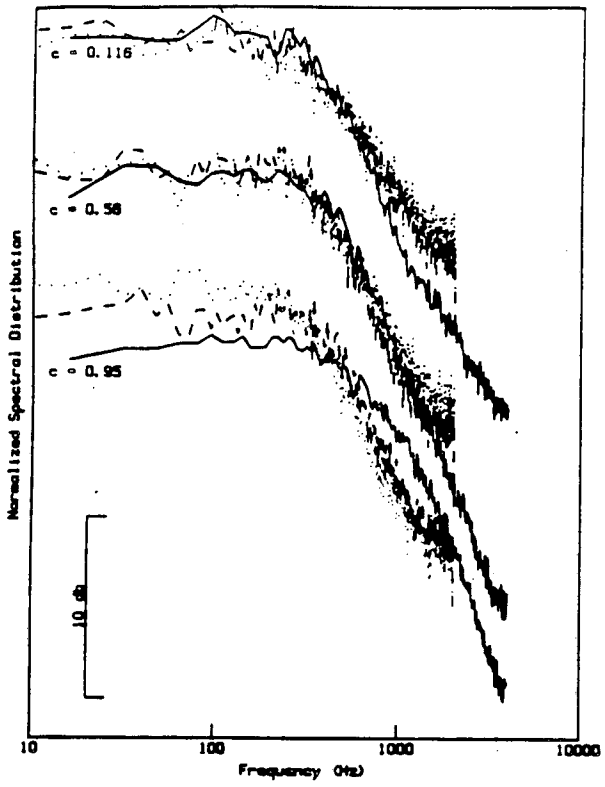

Fig. 5 (a) Comparison of the scalar (intermittency) spectra with the velocity spectra obtained with reference to the laboratory coordinate at three locations in Flame 2 at x = 40.0 mm. ····· u', - - - v' and ——, $\bar{c}$.

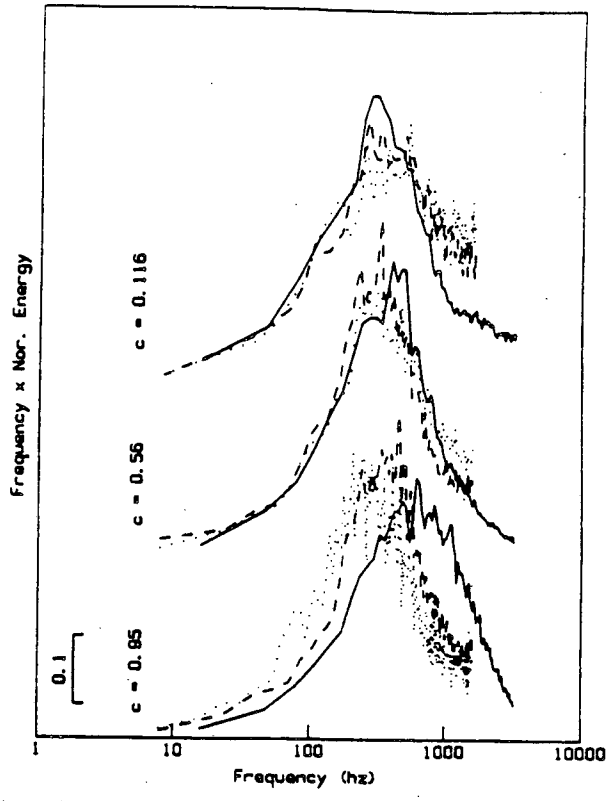

Fig. 5 (b) Comparison of the frequency weighted spectra of Fig. 5 (a).

The normalized energy spectra $E_u(n)$, $E_v(n)$ and $E_c(n)$ for u', v' and scalar $\bar{c}$ respectively obtained at three positions within flame 2 at x = 40.0 mm are compared in Fig. 5(a). The same spectra are plotted again in Fig. 5(b), weighted by the frequency ($nE_u(n)$, $nE_v(n)$, and $nE_c(n)$), to obtain the most energetic frequencies. The results for $\bar{c} = 0.116$ show that the velocity and scalar spectra are similar up to about 600 Hz. At higher frequencies, the spectral distributions for the two velocity components roll-off differently than the scalar spectra. The difference in roll-off is shown in Table II where the the spectral slopes of this set of spectra are listed together with those obtained in flame 2. The spectral slopes are deduced by least square fit of the linear roll off region of the spectra. For the results shown in Fig. 5(a), the linear roll off regions are approximately between 400 and 800 Hz. In Fig. 5(b), the peaks of the energy spectra represent the most energetic frequencies n_e. As can be seen, n_e for the three spectra for $\bar{c} = 0.116$ are all about 300 Hz. The discrepancy between the spectra at n>600Hz is also apparent in this representation which indicates that the velocity fluctuations are more energetic in the higher frequencies than in the scalar fluctuation.

Close to the center of the flame brush ($\bar{c} = 0.56$), the three spectra exhibit similar roll off behavior are consistent up to 1000 Hz. This clearly demonstrate the influence of flame passage on velocity spectra since the contributions of combustion induce acceleration to velocity fluctuations peak at $\bar{c}$=0.5. Comparison of the spectral slope (Table II) also reveals that the slope of v' is more consistent with that of the scalar spectrum. This is not very surprising since the transverse velocity component is closer to the normal of the flame brush and receives a larger contribution from the flame induced velocity jump. The most energetic frequencies deduced from Fig. 5(b) show that n_e for the scalar has shifted to about 400 Hz while those for u' and v' remained relatively unchanged. It is interesting to note that flame passage frequency measured in this flame (10) is about 800 Hz at the flame center. Since the flame passage frequency considers only half of the scalar fluctuation cycle, our results confirm that n_e is indicative of the flame passage frequency.

Towards the hot boundary of the flame brush, ($\bar{c} = 0.95$) the velocity spectra and the scalar spectrum become totally different. One possible explanation is that at this location the probability of encountering flame passage is low and so is the fluctuation intensity of the scalar. The Mie scattering signal therefore contains a relatively larger influence of the photomultiplier noise. This may also explain why the n_e for the scalar spectra is shifted to a higher frequency. The changes in spectra behavior through the flame brush as shown in Fig. 5 are typical of those observed in the v-flames; the scalar and velocity spectra measured elsewhere in flame 1 and in flame 2 all exhibit similar trend.

In Fig. 6(a) are shown the spectra of Fig. 5 transformed with respect to the flame coordinate to obtain spectra for the velocity components normal $E_{u_n}(n)$ and tangential $E_{u_t}(n)$ to the flame brush. The U and V components are transformed into the tangential U_t and normal U_n respectively. The results clearly show changes in the spectral features consequent to this transformation. At $\bar{c} = 0.116$ the three spectra are separated at n > 600 Hz. The difference is shown more clearly in Fig. 6(b). Near the flame center ($\bar{c} = 0.56$), the features of the u_n' and the scalar spectra are similar up to 1000 Hz while the u_t' spectrum is shown with a

Table II

	x (mm) (flame angle)	$\bar{c}$	Spectral Slopes U	V	U_t	U_n	$\bar{c}$
flame 1	30.0 (35°)	0.145	-1.79	-2.11	-1.53	-2.01	-2.07
		0.48	-1.90	-2.12	-1.77	-2.14	-1.85
		0.86	-2.11	-2.20	-2.05	-2.24	-1.56
	40.0 (35°)	0.35	-2.09	-1.73	-1.73	-1.85	-2.02
		0.634	-1.99	-2.01	-1.55	-2.23	-1.50
		0.92	-2.22	-2.22	-1.89	-2.28	-2.17
flame 2	30.0 (18°)	0.13	-1.50	-1.74	-1.29	-1.75	-2.19
		0.31	-1.64	-2.02	-1.35	-2.01	-2.27
		0.8	-1.70	-2.20	-1.50	-2.20	-1.72
	40.0 (26°)	0.116	-1.48	-1.63	-1.24	-1.67	-2.14
		0.56	-1.86	-2.40	-1.87	-2.40	-2.07
		0.95	-2.07	-2.18	-1.57	-1.94	-1.31

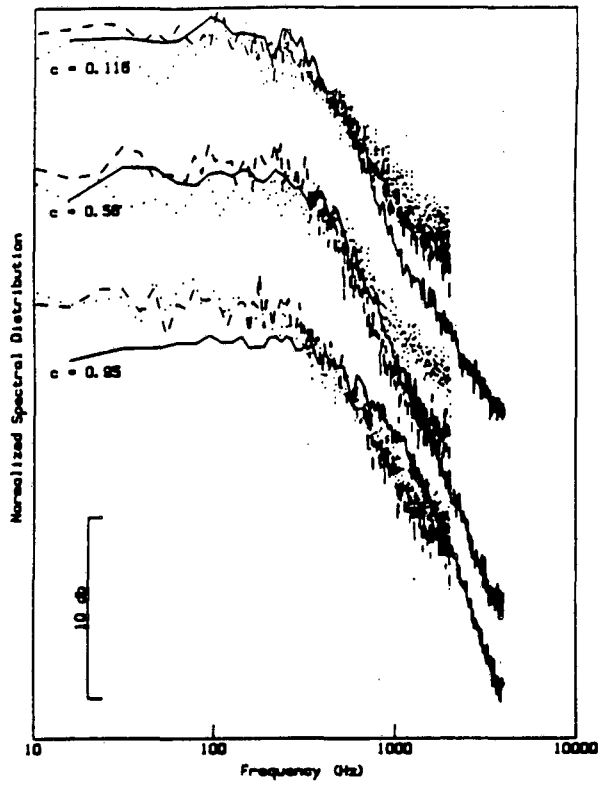

Fig. 6 (a) Comparison of the scalar (intermittency) spectra with the velocity spectra obtained with respect to the flame coordinate at the same positions as those of Fig. 4. $-\cdot-\cdot-\ u_n'$, $\cdots\cdots\ u_t'$, and $\overline{c}$.

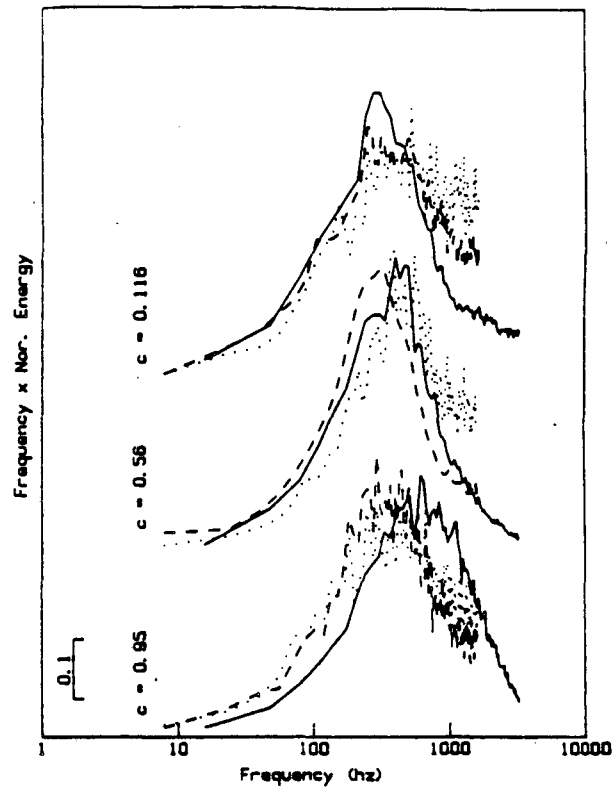

Fig. 6 (b) Comparison of the frequency weighted spectra of Fig. 6 (b)

different roll off characteristics (see also the spectral slopes in Table II). Comparison of the corresponding frequency weighted spectra in Fig. 5(b) and 6(b) shows that the transformation has very little effect on the u_n' spectrum which receive the most significant contributions from the velocity jumps. The most energetic frequencies for the v' and u_n' spectra are about the same. On the other hand, the u_t' spectrum as compared to the u' spectrum seem to have increased energy content in the higher frequency range. Perhaps a decrease in the energy content centered around the most energetic frequency of the scalar spectra (about 400 Hz) may be a more appropriate way to describe this change. This is because even though u' is oblique to the flame brush, it receives some of the contributions from the velocity jumps. After transforming to u_t' the tangential component is insensitive to these jumps because the direction of the velocity jumps are mostly normal to the flame brush. This causes a decrease in the peak u_n' intensity compared to the of u' as shown previously (7). At $c = 0.95$, coordinate transformation again shifted the u_t' spectrum to higher frequency components. The changes are subtle and are shown more clearly in Fig. 5(b) and 6(b). In Fig. 5(b), the u' spectrum peak is at frequencies lower than the v' spectral peak while in Fig. 6(b), the u_t' peak is higher than the u_n' peak. These changes demonstrate that the effects of flame passage is significant even at the boundaries of the flame brush where the probability of encountering flame passage is low.

Since the most energetic frequencies of the scalar spectra is indicative of the flame passage frequencies, it would be illuminating to compare n_e for the velocity spectra with those of the scalar spectra at different positions within the flame zones.

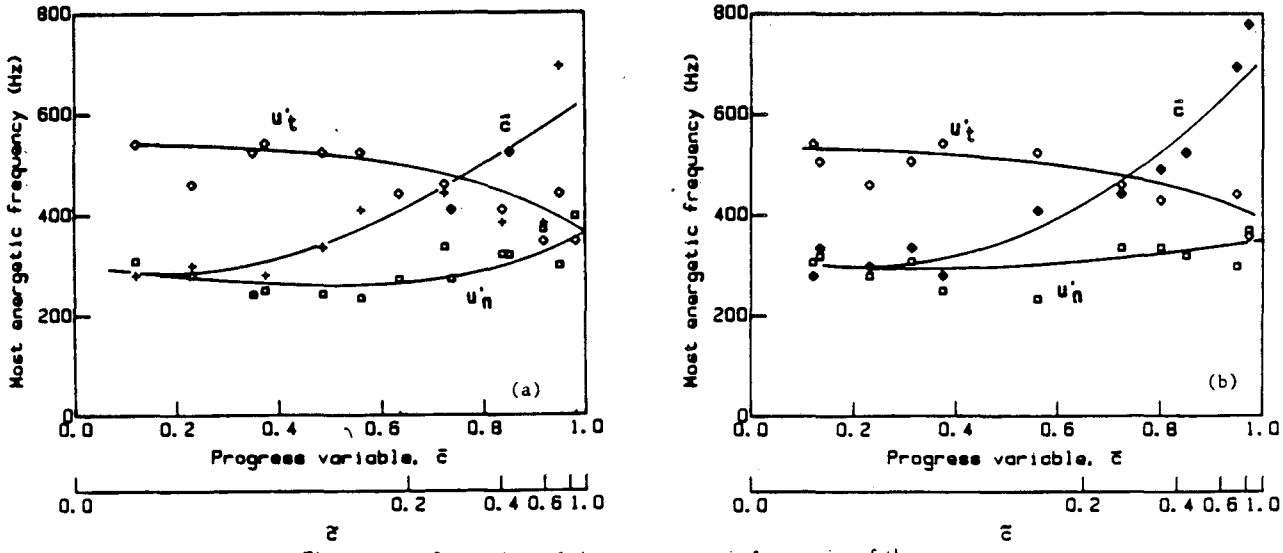

Fig. 7 Comparison of the most energetic frequencies of the intermittency and flame coordinate velocity spectra for (a) Flame 1 and (b) Flame 2.

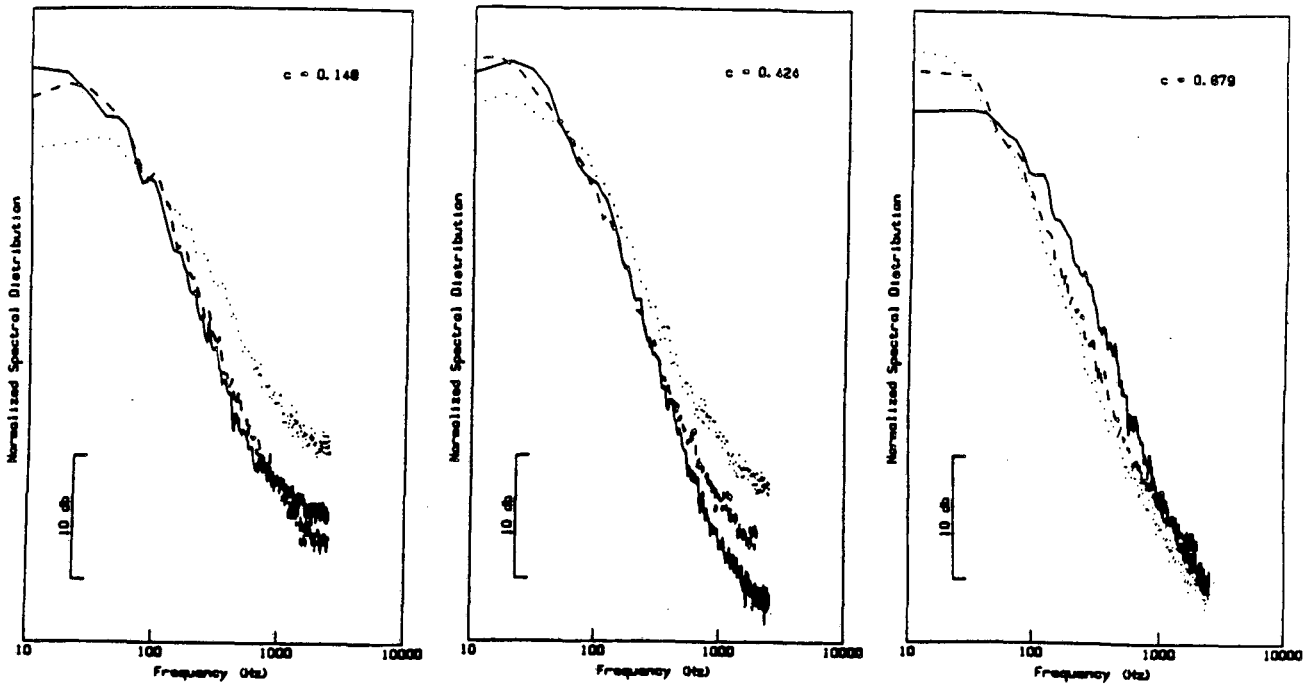

Fig. 8 (a) Comparison of the scalar (intermittency) spectra with the velocity spectra obtained at three locations in Flame 3. ---- u', ····· v' and ——, $\overline{c}$.

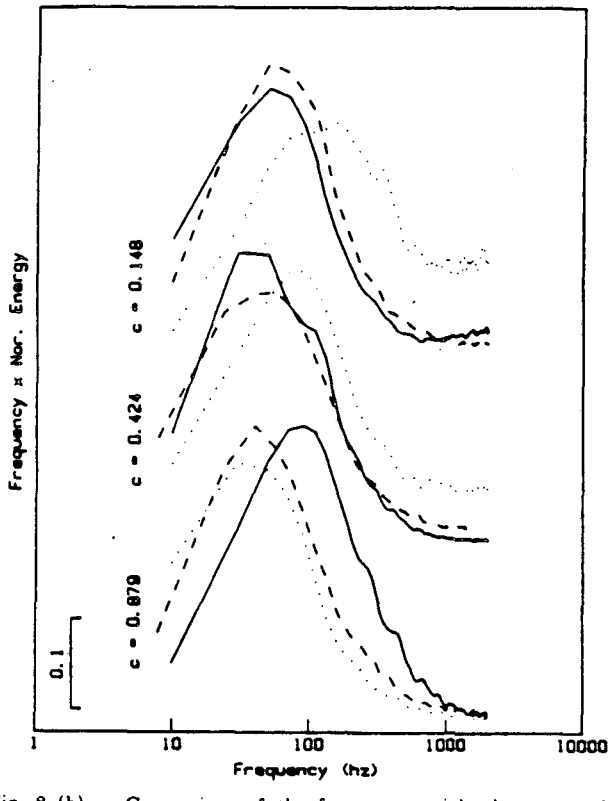

Fig. 8 (b) Comparison of the frequency weighted spectra of Fig. 8 (a).

Shown in Fig. 7(a) and 7(b) are the n_es deduced from the transformed velocity spectra and scalar spectra for Flame 1 and 2 respectively plotted as functions of the conserved scalar $\overline{c}$ and the Favre averaged conserved scalar $\tilde{c}$. Similar trends are observed in both flames. The n_es for the tangential component are at higher frequencies, and tends to decrease slightly towards the product zone ($\overline{c} \rightarrow 1.0$). The most energetic frequencies for the normal component are at lower frequencies and show only a slight decrease at the flame center. The changes in the n_es for the scalar are more significant. Near the reactants ($\overline{c} < 0.5$), they are comparable to those of the normal velocity component. Towards the products, a significant increase is observed in both flames. The cause of this increase is unclear, one possible reason as explained earlier may be due to the increased significance of electronic noise. Another possible cause is the increase in convective mean velocity of flame structures at these locations.

Representative spectra of velocities and scalar measured at three positions within the stagnation flame (flame 3) are compared in Fig. 8. In this flame configuration, the axial velocity component U is normal to the flame zone while the transverse component V is tangential to it. As evident in Fig. 8(a), the spectra in the stagnation flame is quite different from those shown in Fig. 6(a) for the v-flame. Spectral roll-off for all spectra occur at much lower frequencies and the spectral peaks of Fig. 8(b) are situated at frequencies about an order of magnitude lower than those of the v-flames. These frequencies, however, are in accord with the flame passage frequencies. The lower frequencies may be associated with the lowered mean velocities in the stagnation flame as compared to those of the v-flame (see Fig. 4) or may be caused by a change in the length scales. Nevertheless, these spectra clear indicate that the velocity and scalar spectra are coupled. This lends further support to the concept of wrinkled flamelet since our results strongly imply that the flamelets are passive functions of the incident turbulence.

Although it is possible to compare the spectra in wave number space to investigate whether or not the energy containing eddies in the two types of flames are comparable, it is not carried out here due to the fact that the mean velocities in the stagnation flame region is sufficiently low such that the Taylor hypothesis, used to obtain the wave number, would not be accurate. Another concern is the proper velocity to use for computing the wave number of the scalar spectra. Previous studies using two point Rayleigh scattering have shown that the flame structures in the

Table III

		Spectral Slopes		
	$\overline{c}$	U_t	U_n	$\overline{c}$
flame 3	.148	-1.44	-2.01	-2.06
	.424	-1.96	-1.96	-2.09
	.727	-2.12	-1.94	-1.96
flame 4	.096	-1.52	-1.41	-2.27
	.35	-1.67	-1.83	-2.34
	.89	-2.11	-1.93	-2.04

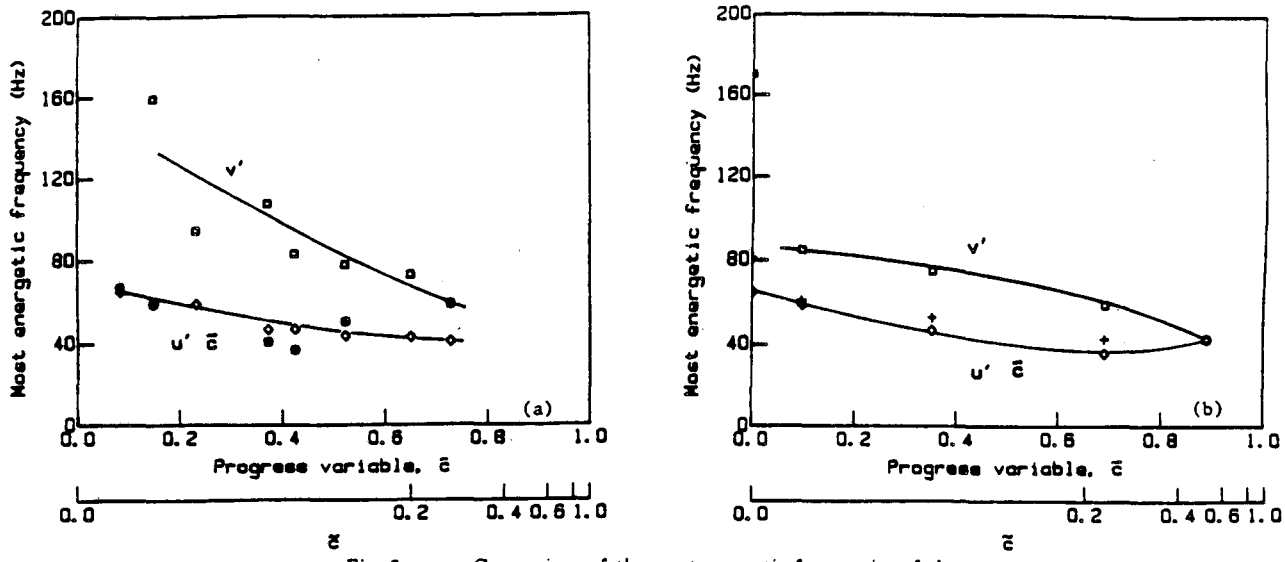

Fig. 9 Comparison of the most energetic frequencies of the intermittency and velocity spectra for (a) Flame 3 and (b) Flame 4.

v-flames are convected tangentially along the flame brush. Therefore, the tangential velocity component would seem to be an appropriate choice for computing the scalar wave number. However, the same logic break down in the stagnation flame because the mean tangential velocity at the centerline where the data were obtained is zero. This and the questionable accuracy of the Taylor hypothesis for the stagnation flame flowfield preclude the comparison of these spectra in wave number space.

The three spectra for $\bar{c} = 0.148$ (Fig. 8(a) and (b)) and the corresponding spectra slopes listed in Table III all confirm that the normal velocity spectra is more consistent with the scalar spectra. Near the flame center ($\bar{c} = 0.424$), the most energetic frequency for the tangential velocity component shifts towards lower frequencies while those of the scalar and normal component remain unchanged (Fig. 8(b). The shifting of n_e for the tangential component towards lower frequency may be associated with the increased contributions of the velocity jumps which tend to be more random due to the restriction of the stagnation plate. Towards the product region ($\bar{c} = 0.848$), the two velocity spectra become almost identical but dissimilar with the corresponding scalar spectra due mainly to the shifting of the scalar spectra to higher frequencies.

The most energetic frequencies in the two stagnation flames are plotted in Fig. 9. Again, the n_es for the tangential velocity component are higher and decrease towards the products zone. More significantly, the n_es for the normal component and the scalar are identical throughout most of the flame zone except at $\bar{c} \rightarrow 0.9$ where the scalar n_e increases. The spectral behavior observed in the stagnation flames such as the changes in the spectral slopes, the shifting to the higher frequency components of the tangential velocity spectra through the flame and the similarities between the scalar spectra and the tangential velocity spectra are identical to the those of the transformed v-flame velocity spectra. This further emphasizes the significance of the velocity data transformed to the flame coordinate for studying velocity data in premixed turbulent flame.

Although our study has clearly demonstrated the influence of flame passage on the velocity spectra. One issue that remains unresolved is the physical process which controls the magnitude of the most energetic frequency of the scalar and hence the turbulence statistical behavior of the normal velocity component. As mentioned earlier, the most energetic frequencies in the v-flames are about an order of magnitude higher than those observed in the stagnation flames while the mean velocities differ only by about a factor of 3.3. The results therefore imply that this difference is not merely due to a decrease in mean velocity. To address this issue properly, the spatial scales of the velocity and scalar fluctuations must be compared to show whether or not the lowering of the roll-off frequencies in the stagnation flame is indeed due to an increase in size of the energy containing eddies. As mentioned earlier, since the application of the Taylor hypothesis in the stagnation point flow is not acceptable, the scales of the velocity fluctuation and flame structures must be measured directly using multi-point diagnostic techniques to obtain space time correlations. For measuring the scales of the flame structures, a tomographic technique based on the principle of aerosol evaporation and multi-point Rayleigh scattering techniques is most appropriate. However, a multi-point LDA technique to determine the velocity spatial scales is under development and will be applied to both flame configurations for further studies of the flame spectral behavior.

CONCLUSIONS

Investigated here is a comparison of the velocity and scalar spectra measured in two premixed turbulent flame configurations (1) rod stabilized v-flame and (2) stagnation flow stabilized planar flame both propagating in approach flow turbulence generated by grid or perforated plate. The velocity spectra were measured using two component laser Doppler anemometry and the scalar spectra were measured using a laser light Mie scattering technique based on the principle of aerosol evaporation through the flame front. Four sets of data have been obtained, two for each configuration using two turbulence generators. The methane/air mixture flow and equivalence ratio conditions of the four flames are the same with $U_\infty = 5.0$ m/s ,$\phi = 0.98$.

To obtain a logical comparison between the results obtained in the two configurations, the data measured in the v-flames are transformed to the coordinate parallel to the local flame orientation. Comparison of the velocity spectra before and after transformation indicates that the effects of transformation is more apparent in the velocity component tangential to the flame region. These effects include changes in the spectral slope and shifting of the most energetic frequencies to higher level. The spectra of the normal velocity component are similar to the scalar spectra which is indicative of the flame passage frequencies. The reason is that the combustion induced velocity jump which occurs after each flame passage is mostly in the normal direction. Consequently, the normal velocity spectra also contain the flame passage spectra.

The spectra measured in the stagnation flames all exhibit similar features which clearly indicate a strong coupling between scalar and velocity spectral behavior. However, the most energetic frequencies are about an order of magnitude higher in the v-flames even though the incident turbulence of the two flame are similar. This difference is not proportional to the difference in the mean velocities implying that the spatial scales in the two flame zones may be different. Since the spatial scales in the stagnation flames cannot be deduced accurately from the time scales, further analysis of the difference in the v-flame and stagnation flame spectra would rely on measurements of the spatial scales.

ACKNOWLEDGEMENTS

This work was supported by the Director, Office of Energy Research, Office of Basic Energy Sciences, Chemical Sciences Division of the U. S. Department of Energy under Contract No. DE-AC-03-76SF00098. One of the authors (IG) was supported by a NATO grant for international collaboration in scientific research. Another author (IGS) is supported by Air Force Office of Scientific Research under Contract No. 84-0124. The authors would also like to acknowledge Mr. Gary Hubbard for developing the data acquisition and analysis software.

REFERENCES

(1) Bray, K. N. C., Libby, P. A., and Moss, J. B. Flamelet Crossing Frequencies and Mean Reaction Rates in Premixed Turbulent Flames. *Combustion Science and Technology* Vol. 41, p. 143 (1984).

(2) Gokalp, I., Shepherd, I. G., and Cheng, R. K. Spectral Behavior of Velocity Fluctuations in Premixed Turbulent Flames. Poster paper presented at the 21st Symposium (International) on Combustion, Munich, Aug. 1986. Also submitted to *Combustion and Flame*.

(3) Peters, N. Laminar Flamelet Concepts in Turbulent Combustion. *21st Symposium (International) on Combustion*, to be published in (1986).

(4) Cheng, R. K. Conditional Sampling of Turbulence intensities and Reynolds Stress in Premixed Turbulent Flames. *Combustion Science and Technology*, Vol. 41, p. 109 (1984).

(5) Cheng, R. K., and Ng, T. T., Velocity Statistics in Premixed Turbulent Flames. *Combustion and Flame*, Vol. 57, p. 156 (1984).

(6) Cho, P., Law, C. K., Hertzberg, J. H. and Cheng, R. K. Structure and Propagation of Turbulent Premixed Flames Stabilized in a Stagnation Flow. To appear in *21th Symposium (International) on Combustion*, The Combustion Institute (1986).

(7) Cheng, R. K., and Shepherd, I. G. Interpretation of Conditional Statistics in Open Oblique Premixed Turbulent Flames. *Combustion Science and Technology* Vol. 49, p. 17 (1986).

(8) Cheng, R. K. and Shepherd, I. G. Intermittency and Conditional Velocities in Premixed Conical Turbulent Flames. To appear in *Combustion Science and Technology* (1987).

(9) Namazian, M, Talbot, L., Robben, F., and Cheng, R. K. Two-point Rayleigh Scattering Measurements in a V-shaped Turbulent Flame. *19th Symposium (International) on Combustion*, The Combustion Institute, p. 487 (1982).

(10) Shepherd, I. G. and Cheng, R. K. An Experimental Evaluation of the BLM Model of the Scalar Field in Turbulent Premixed Flames. Submitted to *Combustion Science and Technology* (1987).

LAWRENCE BERKELEY LABORATORY
TECHNICAL INFORMATION DEPARTMENT
UNIVERSITY OF CALIFORNIA
BERKELEY, CALIFORNIA 94720